SLAC-PUB-1094
(TH) and (EXP)
August 1972

GENERALIZED VECTOR DOMINANCE AND INELASTIC ELECTRON NUCLEON SCATTERING III: THE SMALL ω' REGION*

J. J. Sakurai

Department of Physics
University of California
Los Angeles, California 90024

D. Schildknecht**

Stanford Linear Accelerator Center
Stanford University, Stanford, California 94305

ABSTRACT

The generalized vector dominance model for inelastic electron nucleon scattering is extended to the small ω' region by taking into account the increase of $-t_{min}$ with q^2 in exclusive electroproduction.

(Submitted to Physics Letters.)

*Work supported in part by the U. S. Atomic Energy Commission and the National Science Foundation.

**Permanent address: Deutsches Elektronen Synchrotron, DESY, Hamburg, Germany.

In previous two letters[1,2] we have shown how models based on generalized vector dominance can successfully account for the cross section for inelastic electron-proton scattering at high values of ω' and the neutron-to-proton ratio at low as well as high values of ω'. Our predictions so far cannot, however, accommodate the "threshold behavior" near $\omega' \simeq 1$; specifically the models of Refs. 1 and 2 cannot explain why the transverse cross section $\sigma_T(W, q^2)$ at fixed q^2 <u>increases</u> with W as long as ω' is not too large compared to unity, nor can they explain why the νW_2 curve goes down to zero as $\omega' \to 1$ considerably faster than $\sim (\omega'-1)$. In this letter we discuss how generalized vector dominance can accommodate these striking features when the kinematical limitations due to t_{min} in exclusive electroproduction processes are taken into consideration.

We begin by recalling our predictions for the transverse part of the virtual photon nucleon cross section σ_T for the two alternative models presented in Ref. 2; for model A

$$\sigma_T^{p,n}(W^2, q^2) = \sum_{\rho,\omega,\phi} \left(A_V + \frac{B_V}{\sqrt{K}}\right) \frac{1}{(1+q^2/m_V^2)^2}$$

$$+ \left(A_C + B_C/\sqrt{K} \pm C_C/\sqrt{K}\right) \frac{1}{(1+q^2/m_0^2)} \tag{1a}$$

and for model B

$$\sigma_T^{p,n}(W^2, q^2) = \sum_{\rho,\omega,\phi} \left(A_V + \frac{B_V}{\sqrt{K}}\right) \frac{1}{(1+q^2/m_V^2)^2} + A_C \frac{1}{(1+q^2/m_0^2)}$$

$$+ \left[(B_C \pm C_C)/\sqrt{K}\right]\left[(m_0/2\sqrt{q^2})\left(\frac{\pi}{2} - \tan^{-1}\frac{m_0}{\sqrt{q^2}}\right) + \frac{1}{2}\frac{1}{(1+q^2/m_0^2)}\right], \tag{1b}$$

where the upper and lower sign refer to the proton and neutron target, respectively. In Eqs. (1a, b) in standard notation q^2 and W respectively denote the virtual photon four momentum squared and the virtual photon-nucleon c.m.s. energy; $K \equiv (W^2-m_N^2)/2m_N$ with m_N being the nucleon mass, and $m_{\rho^o,\omega,\phi}$ and m_0 denote the ρ^o, ω, ϕ masses and the onset of the vector state continuum $m_0 = 1.4$ GeV.[1] The numerical values of the constants $A_{V,C}$, $B_{V,C}$ $(V=\rho^o, \omega, \phi)$ and C_C as determined from photoproduction have been given in Ref. 2. Although (1a) and (1b) adequately describe the observed σ_T for large values of $\omega' \equiv 1+W^2/q^2$ (say $\omega' \gtrsim 7$), they considerably overestimate the cross section when ω' becomes small; for example, at $W=2.5$ GeV, $q^2 = 11.0$ GeV^2/c^2, $\omega' = 1.57$, (1a) and (1b) predict 5.25 μb and 7.60 μb, respectively, while the observed σ_T^p is reported to be 1.44 ± 0.18 μb.[3] More generally, (1a) and (1b) are unable to account for the striking threshold behavior mentioned earlier. Clearly, a modification is needed for small values of ω'.

When ω' becomes small and close to unity, q^2 becomes comparable to or greater than W^2. One might speculate that the dynamics of electroproduction processes with q^2 comparable to W^2 is fundamentally different from that of high-energy photoproduction or meson-induced processes; such a view, of course, would be contrary to the spirit of generalized vector dominance. We rather take the point of view that the dynamics is basically similar but that there is an important purely kinematical difference which must be taken into account. Consider

$$\gamma_{\text{virtual}} + N \rightarrow \text{mesonic system} + N \quad . \tag{2}$$

When both W^2 and q^2 become large, with $\omega \equiv \omega' - m_N^2/q^2$ the expression for t_{min} is given by[4]

$$-t_{min} = m_N^2/[\omega(\omega-1)] \tag{3}$$

provided W and $\sqrt{q^2}$ are much larger than the mass of the mesonic system as well as the nucleon mass. This contrasts sharply with the real photon case where for sufficiently high energies, t_{min} is arbitrarily small. According to (3) t_{min} goes to zero for $\omega \to \infty$, but is quite appreciable for small values of ω.

Equation (3) suggests that we may modify our earlier predictions (1a, b) by a multiplicative correction factor

$$e^{bt_{min}} = e^{-\lambda/[\omega'(\omega'-1)]}$$
$$\lambda = b\, m_N^2 \;, \tag{4}$$

where b is identified with the slope parameter for exclusive electroproduction of the type (2).† In this manner we simply eliminate that portion of small t contributions forbidden for purely kinematical reasons.††

The easiest way to test our proposal is to make a logarithmic plot for the ratio of the experimental cross section to the uncorrected prediction (1a) or (1b) against $1/[\omega'(\omega'-1)]$. This is done in Fig. 1 where the experimental points are taken from the separation data of the SLAC-MIT collaboration.[3] It is seen that with the exception of the W = 2 GeV, $q^2 = 1.5\ \mathrm{GeV}^2/c^2$ point all the various data points indeed fall on a straight line to an accuracy of approximately 20% for both models A and B. The best values of λ obtained from eyeball fits to the data points appear to be

$$\lambda = \begin{cases} 1.15 & \text{(Model A)} \\ 1.53 & \text{(Model B)} \end{cases} \tag{5}$$

which correspond to

$$b = \begin{cases} 1.32 & (\mathrm{GeV}/c)^{-2} \\ 1.76 & (\mathrm{GeV}/c)^{-2} \end{cases} \quad . \tag{6}$$

It is somewhat disconcerting that the values of b needed are so small; a priori we might have expected a value such as $b \sim 4\ (\mathrm{GeV}/c)^{-2}$ or greater. We may also mention here that with $\lambda = 1.53$ the modification factor (4) deviates from one by less than 4% for $\omega' \gtrsim 7$.

In Fig. 2 we show the results obtained for σ_T^p according to the unmodified and the t_{min} corrected models A and B in comparison with the experimental data.[3] As seen on Fig. 2, the modification of the original prediction is, of course, largest for the smallest value of W considered, W = 2.5 GeV, for which the increase of $-t_{min}$ with q^2 is most strongly felt.

In Fig. 3 we plot σ_T^p as a function of W^2 for fixed q^2. For low values of q^2, σ_T^p decreases as W increases just as in high energy photoproduction; however, when q^2 is so high that ω' becomes close to unity, σ_T^p at first increases as W increases. All these features are adequately reproduced in our model.

Figure 4 shows the transverse contribution to νW_2^p:

$$\nu W_{2T}^p \equiv \nu W_2^p/(1+R_p) \tag{7}$$

for various values of q^2. Our t_{min} corrected model predicts that as $\omega' \to 1$, the transverse contribution to νW_2^p goes as

$$(\omega'-1)^\beta \ \exp(-\lambda/\omega'(\omega'-1)) \tag{8}$$

with $\beta = 1$ for Model A and $\beta = 1/2$ for Model B. In contrast, most phenomenological fits to the νW_2^p curve assume a power behavior[6] $(\omega'-1)^N$ with N =3 as the most likely choice.[3] If at very large values of t the differential cross section for (2) went down as a negative power of t, rather than as e^{bt}, our basic philosophy could be reconciled with the more conventional power behavior. At this stage, however, it is difficult to tell whether the $(\omega'-1)^3$ behavior is preferred to our exponential behavior (8) for ω' very close to unity.

To summarize, our original no-adjustable-parameter predictions for σ_T appropriate for large ω' can be successfully extended to kinematical regions with small ω' by introducing just one parameter. It is gratifying that this simple modification based on the t_{min} effect is sufficient to account for the gross features of the data even near "threshold" $\omega' \simeq 1$. It is likely that a more complete understanding of the small ω' region becomes possible only when we learn more about the nature of specific final states produced in inelastic electron nucleon collisions.

FOOTNOTES

† If the target nucleon is also excited (to a state of mass m*) t_{min} appearing in Eq. (3) has to be replaced by[4]

$$-t_{min} = \frac{+\,m_N^2}{\omega(\omega-1)} + \frac{(m^{*2} - m_N^2)}{(\omega-1)} \quad .$$

For simplicity we do not consider the resulting modification. To facilitate comparison with our earlier papers we prefer to work with ω'; as long as q^2 is much larger than m_N^2, there is no difference between ω and ω'.

†† Precisely this proposal was made by Ritson.[5] The importance of t_{min} in inelastic electron-proton scattering in the scaling region was first recognized by West.[4]

REFERENCES

1. J. J. Sakurai and D. Schildknecht, Phys. Letters 40B (1972) 121.
2. J. J. Sakurai and D. Schildknecht, University of California, Los Angeles preprint UCLA/72/TEP/57 (1972).
3. G. Miller et al., Phys. Rev. D5 (1972) 528.
4. G. West, Phys. Rev. Letters 24 (1970) 1206.

   J. D. Sullivan, NAL preprint, NAL-THY-24 (1971).
5. D. M. Ritson, Phys. Rev. D3 (1971) 1267.
6. S. D. Drell and T.-M. Yan, Phys. Rev. Letters 24 (1970) 181.

FIGURE CAPTIONS

1. The ratio of the measured transverse cross section[3] σ_T^p to our unmodified predictions according to Eqs. (1a, b) as a function of $1/\omega'(\omega'-1)$.
2. σ_T^p as a function of q^2 for fixed W. The theoretical curves show the results obtained from Eqs. (1a, b) without t_{min} correction and after modification with the multiplicative factor from Eqs. (4) and (5).
3. σ_T^p as a function of W^2 for fixed q^2.
4. The transverse contribution to the proton structure function νW_2^p as a function of ω' for various values of q^2. The scaling limit is also indicated.

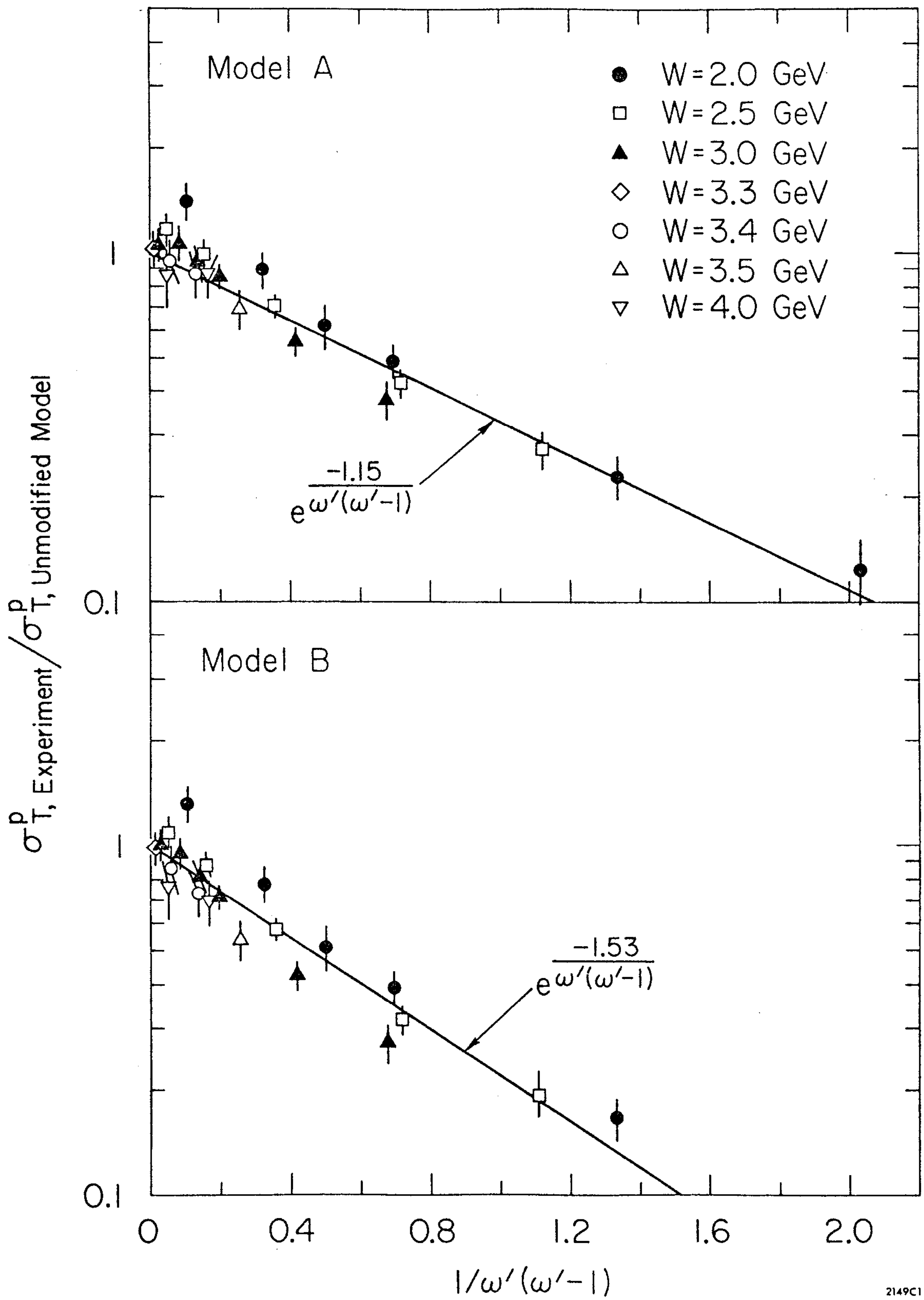
Model A
W=2.0 GeV
W=2.5 GeV
W=3.0 GeV
W=3.3 GeV
W=3.4 GeV
W=3.5 GeV
W=4.0 GeV
e^{-1.15/ω'(ω'-1)}
Model B
e^{-1.53/ω'(ω'-1)}
1
0.1
1
0.1
0
0.4
0.8
1.2
1.6
2.0
1/ω'(ω'-1)
σ^p_{T, Experiment}/σ^p_{T, Unmodified Model}
2149C1

Fig. 1

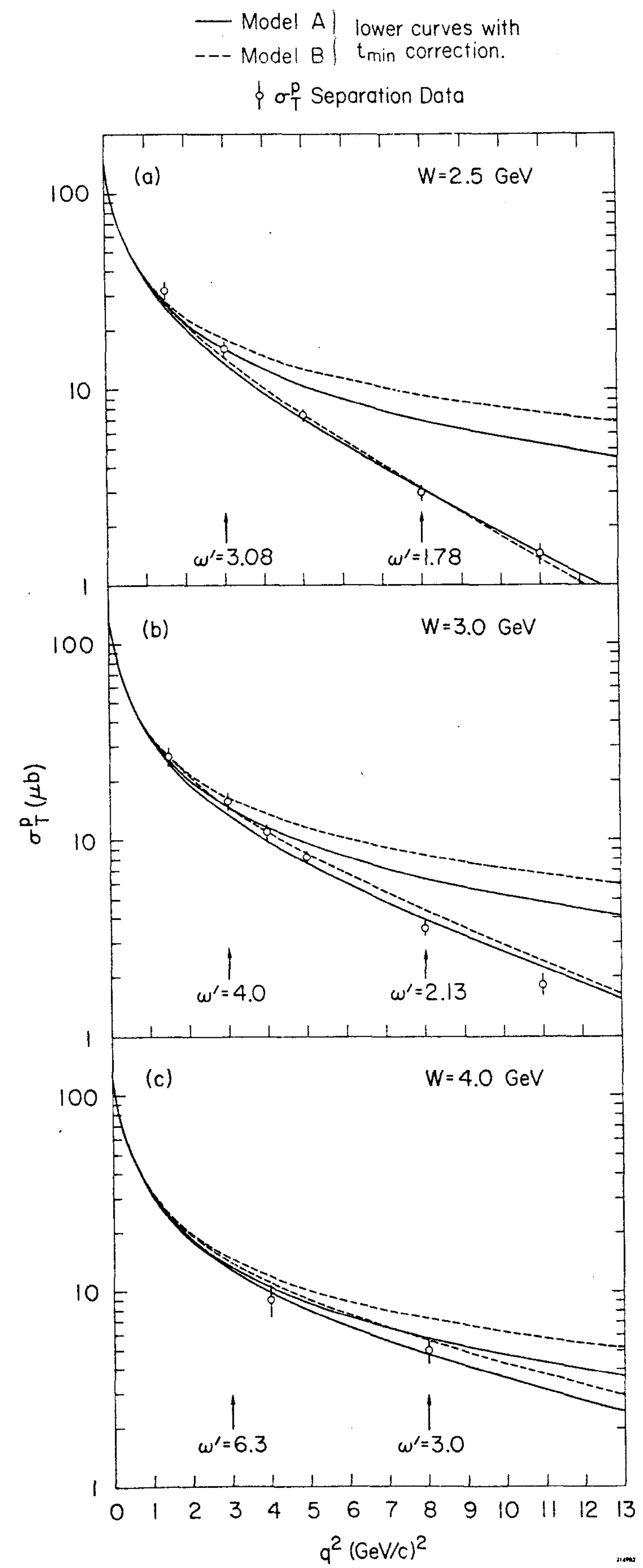
Model A
Model B
lower curves with t_{min} correction.
σ_T^p Separation Data
(a)
W=2.5 GeV
100
10
1
ω′=3.08
ω′=1.78
(b)
W=3.0 GeV
ω′=4.0
ω′=2.13
σ_T^p (μb)
(c)
W=4.0 GeV
ω′=6.3
ω′=3.0
0 1 2 3 4 5 6 7 8 9 10 11 12 13
q^2 (GeV/c)^2

Fig. 2

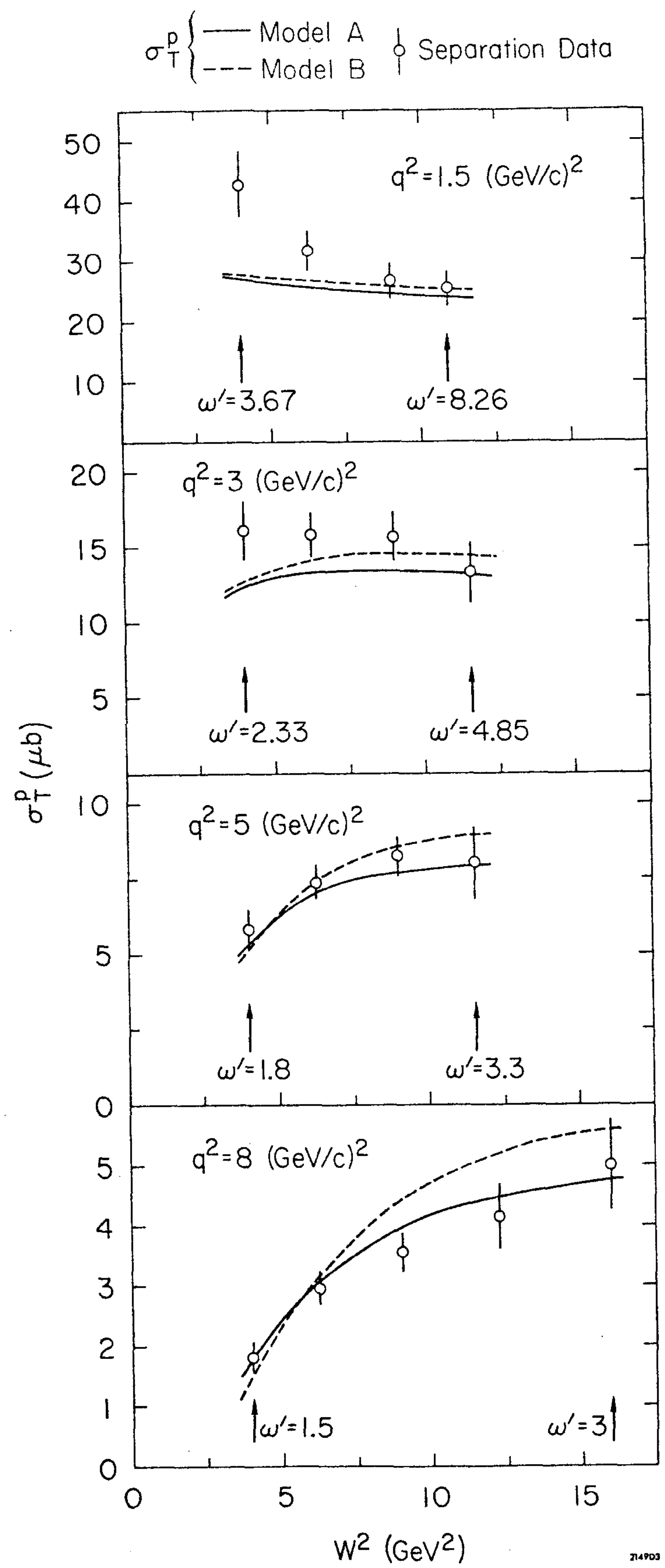
σ_T^p — Model A
--- Model B
Separation Data
q^2=1.5 (GeV/c)^2
ω′=3.67
ω′=8.26
q^2=3 (GeV/c)^2
ω′=2.33
ω′=4.85
q^2=5 (GeV/c)^2
ω′=1.8
ω′=3.3
q^2=8 (GeV/c)^2
ω′=1.5
ω′=3
σ_T^p (μb)
W^2 (GeV^2)
2149D3

Fig. 3

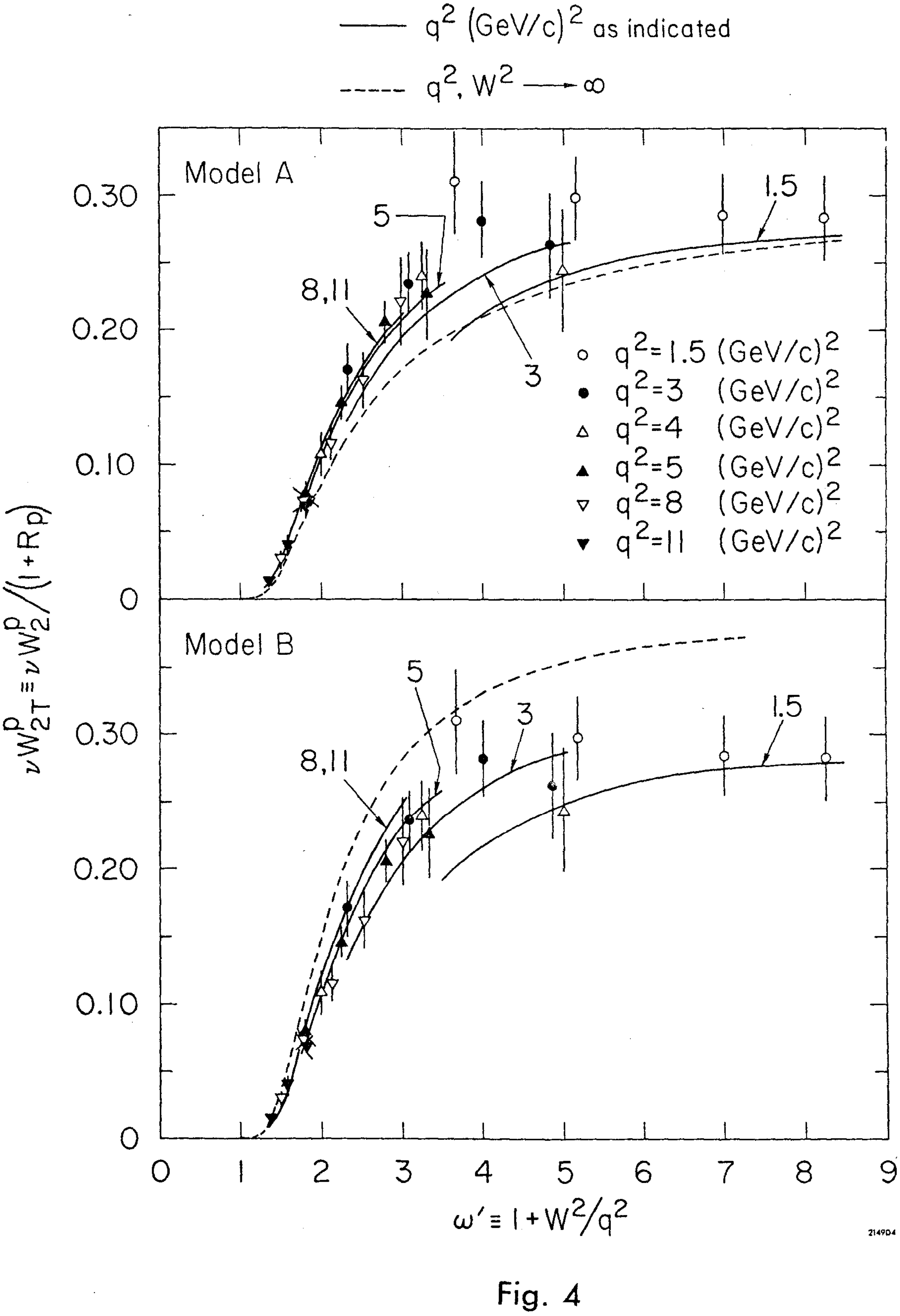

q2 (GeV/c)2 as indicated
q2, W2 → ∞
Model A
Model B
5
8,11
3
1.5
q2=1.5 (GeV/c)2
q2=3 (GeV/c)2
q2=4 (GeV/c)2
q2=5 (GeV/c)2
q2=8 (GeV/c)2
q2=11 (GeV/c)2
νW2Tp ≡ νW2p/(1+Rp)
ω′ ≡ 1+W2/q2
0.30
0.20
0.10
0
0 1 2 3 4 5 6 7 8 9
2149D4

Fig. 4